

M. GALARZA<sup>1</sup>, ✉  
J. MORENO<sup>1</sup>  
M. LOPEZ-AMO<sup>1</sup>  
I. CHRISTIAENS<sup>2</sup>  
D. VAN THOURHOUT<sup>2</sup>  
R. BAETS<sup>2</sup>

## Simple low-loss waveguide bends using ARROW effect

<sup>1</sup>Electric and Electronic Department, Public University of Navarre, Campus of Arrosadia, 31006 Pamplona, Navarre, Spain

<sup>2</sup>Department of Information Technology, Ghent University-IMEC, St.-Pietersnieuwstraat 41, 9000 Ghent, Belgium

Received: 15 October 2004 /

Revised version: 6 December 2004 /

Published online: 17 March 2005 • © Springer-Verlag 2005

**ABSTRACT** A new concept for reducing bend loss in dielectric planar waveguides is presented. It is based on the introduction of a set of antiresonant reflecting optical waveguides (ARROWs) on the outside of the bent core and defined in the same fabrication step as the main bend. It has been ascertained by simulation that the bending loss can be significantly reduced. The method is compatible with other bend-loss-reduction strategies, as well as with different waveguiding structures, such as rib and buried waveguides and fibers.

PACS 42.82.Et

Curved waveguides are key components in photonic integrated circuits and are mainly used to change the direction of light or to introduce a lateral displacement. In order to achieve a high packing density in limited chip areas, it is mandatory to minimize the bend radius as much as possible, without introducing significant bend loss. Unfortunately, bend loss increases almost exponentially with decreasing radius of curvature.

There exist three major methods for reducing bend loss. One method is the introduction of refractive-index changes in order to increase the relative index difference between the core and the cladding [1] or to accelerate the phase fronts at the outer side of the bend [2]. A second method replaces the bend by a coherently coupled multisection bend to reduce the loss [3]. The introduction of an isolation trench [4], corner mirror [5], or outrigger waveguide of higher refractive index [6] on the outside of the bent core decreases the evanescent modal field more rapidly in the region between the waveguide core and the apparent origin of radiation, so that radiation loss is also reduced. Nevertheless, most of these strategies involve additional processing steps during fabrication.

In this paper, we propose a novel and straightforward technique for reducing the bend radius by making use of ARROW (antiresonant reflecting optical waveguide) structures [7, 8]. The concept has the advantage that it does not require any

extra processing step. A set of  $N$  concentric waveguides on the outer side of the bend and defined in the same step as the main waveguide (Fig. 1) are designed to provide antiresonant reflection to the radiated light. A ray radiated from the bend will undergo multiple reflections at each interface defined by the ARROW structure, and for an appropriate design the rays coming back to the curved waveguide have the same phase, interfering constructively and coupling back to the propagating mode. Figure 1a shows the electric field plot of light propagating in a bend of constant radius. We observe a huge power leakage for the standard bend mode. On the contrary, the corresponding ARROW curve with four lateral waveguides of

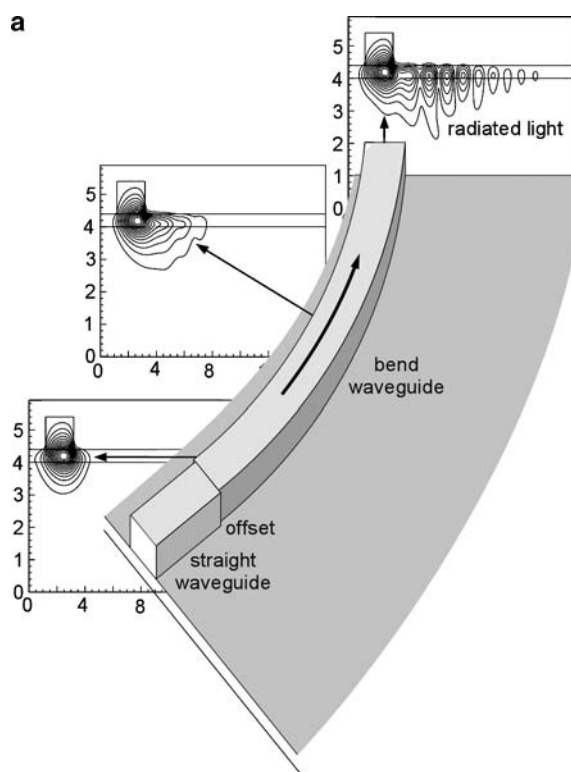


**FIGURE 1** Schematic drawing of the proposed bend concept. **a** Propagation field in a standard bend waveguide; **b** propagation field along the same waveguide bend having lateral ARROW waveguides

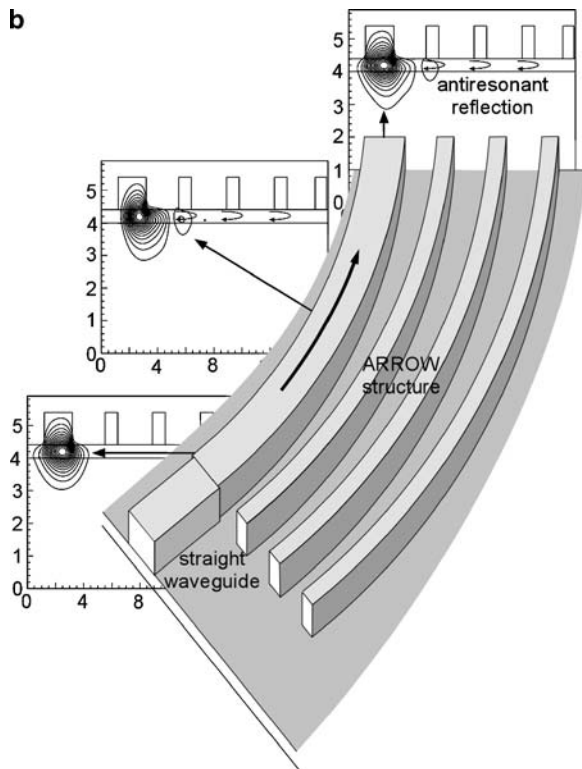


FIGURE 1 Continued

Fig. 1b shows almost no power leakage to the outside of the bend.

For the simulations, we assume a typical InP/InGaAsP low-confinement rib structure consisting of a quaternary core layer of refractive index  $n_{co}$  and thickness  $h_{co}$  on an InP substrate and with a top InP cladding layer with a thickness  $h_{cl}$ . The waveguide has a width  $w$  and is etched down to the top of the quaternary layer. The  $N$  lateral rib waveguides, structurally identical to the main waveguide, are also shown in Fig. 2. Each of them is  $w_i$  wide and is separated by a distance  $d_i$  from the previous rib.

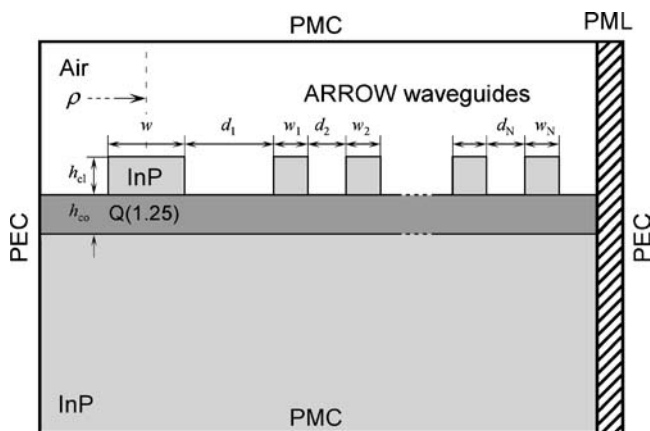


FIGURE 2 Cross section of the ARROW bend waveguide and detail of the boundaries used in the simulation: PEC and PMC stand for perfect electric and magnetic conductors, respectively; PML is a perfectly matched layer, which absorbs the radiation in the bend

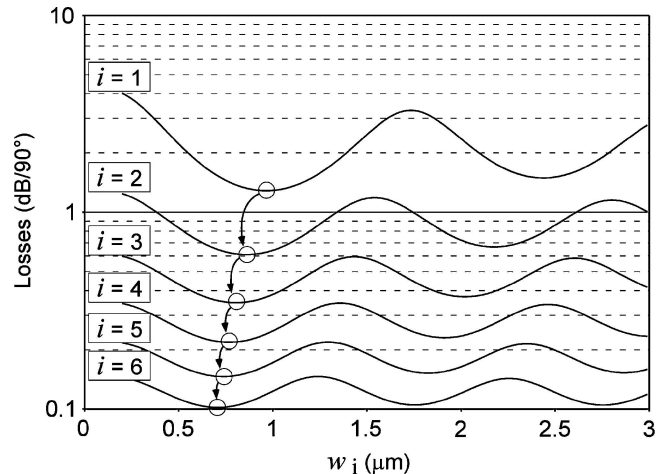


FIGURE 3 Bending loss as a function of the width  $w_i$  of each of the  $N = 6$  lateral waveguides. The first minimum of the quasi-periodic response is used in the sequential design. The choice of  $d_i$  corresponds to minimum bend loss

A commercial three-dimensional complex mode solver (*Fimmwave* [9]) was used to design the optimal dimensions for the lateral ARROW waveguides and quantify the improvement achieved. The fully vectorial mode solver is based on the film mode matching method [10], which, in the case of curved waveguides, solves the Maxwell equations in cylindrical coordinates. A perfectly matched layer (PML) located at the outer side of the bend absorbs the power leaked out of the bend, avoiding any parasitic reflection, thanks to the imaginary part of its thickness. Since no radiation is produced towards the other three transverse directions in the low-confinement rib waveguide considered, perfect electric and magnetic conductors are used as boundary conditions for these. With this scheme the mode solver allows us to calculate the losses of the different modes and their propagation constants.

For each lateral rib two parameters have to be defined: its width  $w_i$  and the gap  $d_i$ . The  $N$  ARROW waveguides were sequentially optimized by scanning for the minimum loss point in the two-dimensional parameter space ( $w_i, d_i$ ). We consider a waveguide of width  $w = 3 \mu\text{m}$ , a core with index  $n_{co} = 3.36$  (Q1.25) and thickness  $h_{co} = 600 \text{ nm}$ , a cladding and substrate index  $n_{cl} = 3.17$ , a cladding thickness  $h_{cl} = 300 \text{ nm}$ , and an excitation wavelength  $\lambda = 1.55 \mu\text{m}$  for the analysis. Figure 3 shows the bending loss, in  $\text{dB}/90^\circ$ , as a function of the width  $w_i$  of each lateral waveguide, for a radius of  $500 \mu\text{m}$  and for TE polarization. For each rib the choice of  $d_i$  corresponds to minimum bend loss. As shown we considered  $N = 6$  lateral waveguides.

A quasi-periodic Fabry–Pérot-like response, typical for antiresonant reflecting structures, is obtained. Circles surrounding the minimum loss points for the first periods represent the starting points for the consecutive scans. In each step, a significant loss reduction is obtained. A slight reduction of the oscillation is observed for successive periods due to the decrease of the radial component of the wave number with the radius [11].

Table 1 shows, for several radii, the calculated pairs of parameters  $w_i, d_i$  for  $N = 6$  lateral waveguides. We see that the optimal rib widths and the gaps decrease with decreasing radius, and that most dimensions are sub-micrometer, even for

$\rho$	300	400	500	600	700	800	900
$d_1$	1.9	2.43	2.98	3.51	4.12	4.75	5.29
$w_1$	0.91	0.94	0.97	1	1.01	1.01	1.04
$d_2$	0.74	0.86	0.96	1.06	1.14	1.14	1.24
$w_2$	0.8	0.85	0.86	0.88	0.89	0.94	0.94
$d_3$	0.56	0.63	0.72	0.79	0.85	0.9	0.98
$w_3$	0.74	0.78	0.81	0.83	0.85	0.86	0.86
$d_4$	0.47	0.54	0.59	0.65	0.69	0.78	0.81
$w_4$	0.69	0.73	0.77	0.79	0.81	0.81	0.83
$d_5$	0.41	0.48	0.52	0.57	0.61	0.67	0.67
$w_5$	0.67	0.7	0.74	0.76	0.78	0.78	0.82
$d_6$	0.36	0.43	0.47	0.51	0.56	0.6	0.61
$w_6$	0.65	0.68	0.71	0.74	0.75	0.77	0.79

**TABLE 1** Widths ( $w_i$ ) and gaps ( $d_i$ ) of the lateral ARROW waveguides for several radii and designed in the first minimum antiresonant working point. All units are in  $\mu\text{m}$

$\rho$	300	400	500	600	700	800	900
$d_1$	1.9	2.43	2.98	3.51	4.12	4.75	5.29
$w_1$	2.24	2.35	2.44	2.52	2.56	2.6	2.65
$d_2$	1.92	2.18	2.39	2.6	2.76	2.94	3.1
$w_2$	1.72	1.83	1.92	1.99	2.06	2.08	2.13
$d_3$	1.38	1.57	1.73	1.85	1.98	2.09	2.18
$w_3$	1.54	1.63	1.7	1.78	1.82	1.88	1.94
$d_4$	1.14	1.3	1.45	1.56	1.68	1.74	1.85
$w_4$	1.46	1.52	1.58	1.64	1.7	1.76	1.78
$d_5$	0.96	1.13	1.26	1.37	1.46	1.55	1.63
$w_5$	1.36	1.45	1.5	1.57	1.6	1.65	1.69
$d_6$	0.9	1.01	1.13	1.22	1.3	1.4	1.46
$w_6$	1.3	1.38	1.45	1.5	1.56	1.58	1.63

**TABLE 2** Widths ( $w_i$ ) and gaps ( $d_i$ ) of the lateral ARROW waveguides for several radii and designed in the second minimum antiresonant working point. All units are in  $\mu\text{m}$

the biggest radius  $\rho = 900 \mu\text{m}$ . Such small features may be difficult to achieve with standard photolithography. However, taking into account the periodicity of the Fabry–Pérot-like response of the ARROW structure, we can shift the working point to the minimum of the second period in order to increase the minimum waveguide features. Figure 4 shows the result for a new set of scans. Circles now show the successive minima found in the second period. Since the Fabry–Pérot response was not perfectly periodic due to the curve effect, the bend-loss reduction is lower than in the optimum structure, but still considerable. Design results are shown in Table 2. The minimum feature, for the smallest radius, is now  $0.9 \mu\text{m}$ , while the rest are higher than  $1 \mu\text{m}$ , perfectly achievable with standard lithographic techniques.

Figure 5 shows the calculated radiation losses of the waveguide, as a function of bending radius  $\rho$  and for different numbers  $N$  of lateral ARROW waveguides for the first (Fig. 5a) and second (Fig. 5b) minimum point designs. In the former, the loss in dB is reduced by a factor of 10 using only three lateral ribs, and keeps on decreasing significantly using the other three ribs. The improvement factor is higher for large radii than for small ones. From an integration point of view, we

observe that for a given loss, it is possible to reduce the radius of the bend by a factor close to 2, which means that the area can be reduced by a factor close to 4. By increasing the number of ribs further, the area-reduction ratio could still be increased.

From the results provided by the second minimum design (Fig. 5b), we see a lower improvement compared to the previous structure. A loss-reduction factor higher than 10 dB for a given radius was achieved using all the six lateral ribs. Here

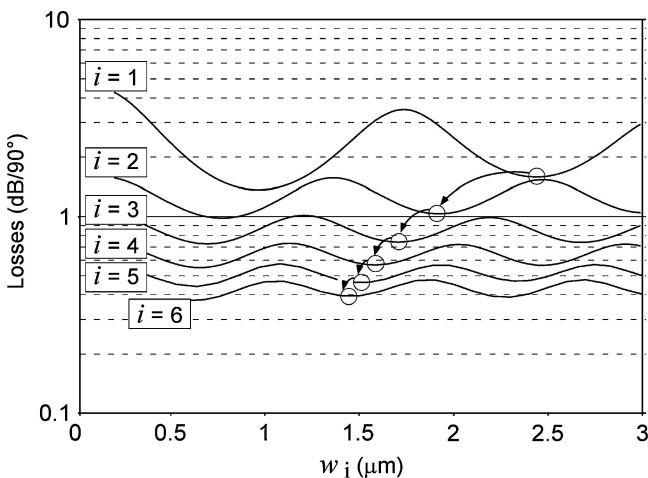


**FIGURE 4** Bending loss as a function of the width  $w_i$  of each of the  $N = 6$  lateral waveguides. The second minimum of the quasi-periodic response is used in the sequential design. The choice of  $d_i$  corresponds to minimum bend loss

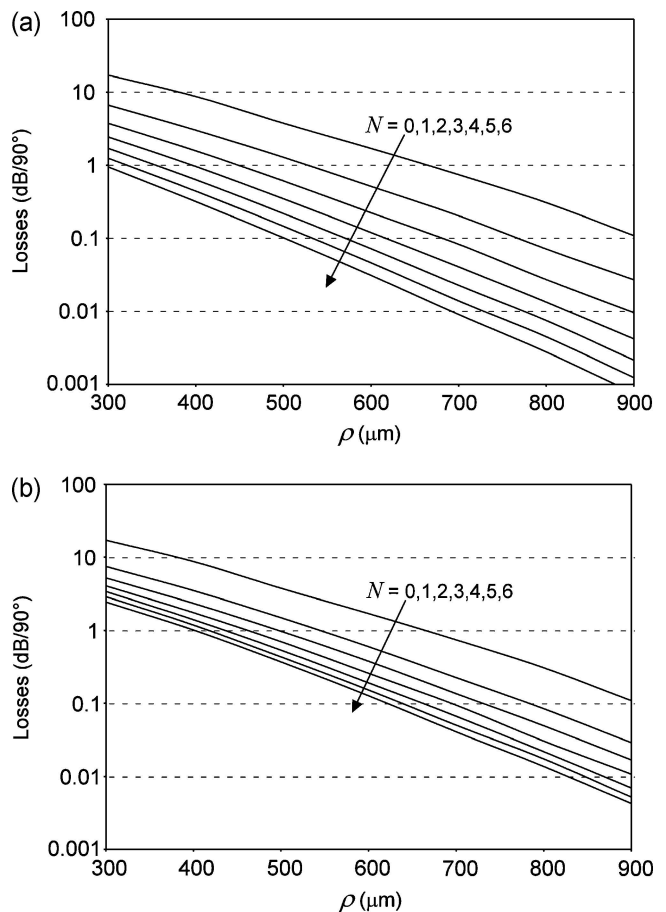


**FIGURE 5** Bending loss per  $90^\circ$  as a function of bend radius and number of lateral waveguides for **a** first minimum and **b** second minimum working point designs

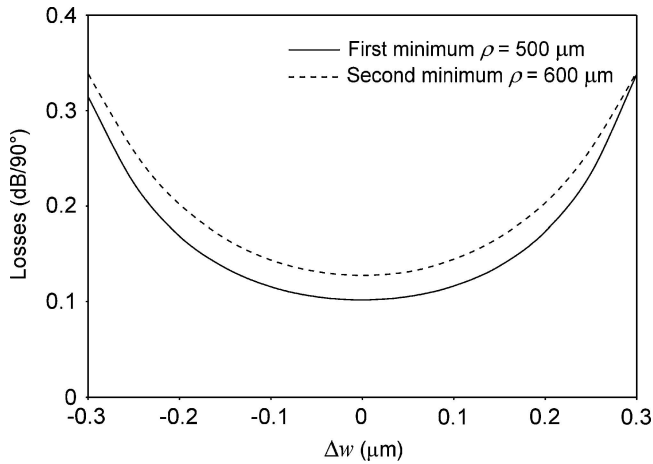


**FIGURE 6** Calculated loss as a function of general variation in the widths of the lateral ARROW waveguides for the two proposed designs

also, increasing the number of lateral ARROW waveguides will lead to additional loss reduction.

As mentioned above, the simulated designs were optimized for TE polarization. Due to the fact that the waveguide is shallowly etched, TM polarization presents lower radiation losses than the minimum obtained for TE in any of the two ARROW bend structures and even in the standard bend, making them polarization independent.

The performance of ARROW bends as a function of variation in the width of the lateral ribs has also been studied. It is very common to have this kind of variation during the processing of the devices. Figure 6 shows the calculated radiation losses of the two proposed ARROW bend structures designed around the 0.1-dB loss working point and having  $N = 6$  lateral ribs, as a function of a general variation in the width of the lateral ribs. We observe a smooth increase of the loss by less than 1 dB in a safe lithographic range.

Next to the radiation loss, a curved waveguide also exhibits losses at the transition between the straight and the bend waveguides caused by the shift of the mode field in the bend waveguide. The transition loss can be minimized by introducing a lateral offset between the straight and the curved waveguides in order to align the field maxima. Figure 7 shows the optimized transition losses as a function of the radius for the two designs proposed in this work, which are compared with the transition loss for a standard bend without any lateral ARROW waveguide. A general loss reduction is obtained for the new structures along the considered radii range. This improvement has to be added to the radiation-loss reduction demonstrated above.

In conclusion, we have proposed and analyzed a new bend concept based on the ARROW effect provided by a set of

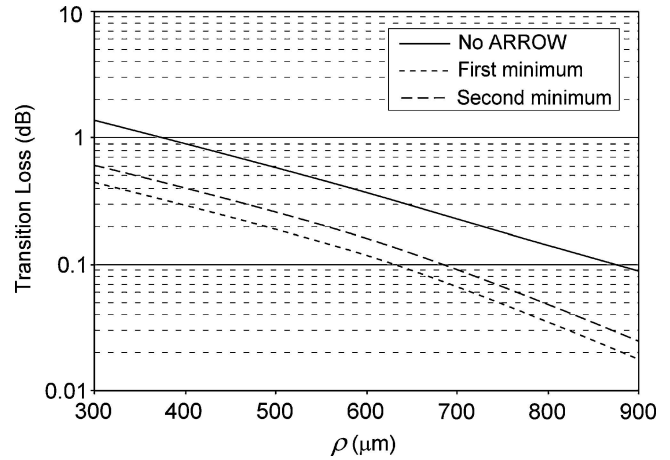


**FIGURE 7** Calculated minimum transition losses of the standard bend and the two proposed new ARROW bend structures with  $N = 6$  lateral waveguides

properly designed waveguides. These are defined in the same processing step as the central waveguide and, thus, do not require any additional processing. Applicability to a typical InP-based waveguide structure has been analyzed and a significant bending-loss reduction has been observed. The concept is compatible with other bending-loss-reduction techniques using one photolithographic step, such as S-shaped bends, continuous waveguide widening and bending, and even multisectional bends [3], as well as with most of the transition loss reduction techniques. It is also applicable to buried structures and single-mode fibers.

**ACKNOWLEDGEMENTS** This work was supported by the European Sixth Framework Programme under a Marie Curie grant, and Ministerio Español de Ciencia y Tecnología under Project Nos. TIC2001-0877-C02-02 and TEC2004-05936-C02-01.

## REFERENCES

- 1 R.A. Jarvis, J.D. Love, F. Ladouceur, *Electron. Lett.* **33**, 892 (1997)
- 2 S. Tomljenovic-Hanic, J.D. Love, A. Ankiewicz, *Electron. Lett.* **38**, 220 (2002)
- 3 J.-J. Su, W.-S. Wang, *IEEE Photon. Technol. Lett.* **14**, 1112 (2002)
- 4 C. Seo, J.C. Chen, *J. Lightwave Technol.* **14**, 2255 (1996)
- 5 L.H. Spiekman, Y.S. Oei, E.G. Metaal, F.H. Groen, P. Demeester, M.K. Smit, *IEEE Proc.: Optoelectron.* **142**, 61 (1995)
- 6 S.N. Radcliffe, T.P. Young, *IEEE J. Sel. Area Commun.* **6**, 1169 (1988)
- 7 M.A. Duguay, Y. Kokubun, T.L. Koch, L. Pfeiffer, *Appl. Phys. Lett.* **49**, 13 (1986)
- 8 T. Baba, Y. Kokubun, *IEEE Photon. Technol. Lett.* **1**, 232 (1989)
- 9 *Fimmwave* (Photon Design) [<http://www.photond.com>]
- 10 A.S. Sudbo, *IEEE Photon. Technol. Lett.* **5**, 342 (1993)
- 11 E.C.M. Pennings, PhD Thesis (1990) [ISBN 90-9003413-7]